Intravascular Elimination of Circulating Tumor Cells and Cascaded Embolization with Multifunctional 3D Tubular Scaffolds

Yijing Chen,†[a] Cuiwen Li,†[a] Jinghui Yang,†[b] Ming Wang,[d] Yike Wang,[a] Shibo Cheng,[a] Weihua Huang,[a, c] Guohua Yuan,*[b] and Min Xie*[a]

[a] College of Chemistry and Molecular Sciences, Wuhan University, Wuhan 430072, China

[b] School and Hospital of Stomatology, Wuhan University, Wuhan 430079, China

[c] Department of Hepatobiliary and Pancreatic Surgery, Zhongnan Hospital of Wuhan University, Wuhan 430071, China

[d] Department of Clinical Laboratory, Renmin Hospital of Wuhan University, Wuhan 430060, China

Correspondence

E-mail: mxie@whu.edu.cn; yuanguohua@whu.edu.cn

Materials and Instruments. Ni foam was purchased from Kunshan Jiayisheng Electronics Co. Ltd. Silver nanowires (Ag NWs, 35–45 nm in diameter, 10–20 μm in length) were obtained from Zhejiang Kechuang Advanced Materials Tech Co., Ltd. (Hangzhou, China). Indwelling needles (18 G, 1.31 mm × 29 mm) were purchased from Fenglin Medical Appliances Co., Ltd. (Jiangxi, China). CD326 biotin-labeled mouse anti-human anti-EpCAM monoclonal antibody and 1, 1-dioctadecy l-3, 3, 3, 3-tetramethylindocarbocyanine perchlorate (DiI) was ordered from ThermoFisher. Gelatin, bovine serum albumin (BSA), DyLight 488 conjugated goat anti-mouse secondary antibody, streptavidin (SA), Calcein-AM, and propidium iodide (PI) and Hoechst 33258 solution were received from Sigma-Aldrich. Anti-EpCAM antibody (ab216832), FITC-labeled mouse anti-human cytokeratin (FITC-CK), and PE-labeled mouse anti-human CD45 (PE-CD45) were obtained from Abcam Company. 808 nm laser was purchased from Hi-Tech Optoelectronics Co. Ltd. HepG2 cells was ordered from Procell Life Science & Technology Co., Ltd. (Wuhan, China). VX2 cells was purchased from Qingqi Biotechnology Development Co., Ltd. (Shanghai, China). All other chemicals were supplied by Shanghai Chemical Reagent Company. Female New Zealand rabbits were raised in the Animal Experiment Center of Wuhan University (Wuhan, China).

SEM images were obtained using a Zeiss Sigma field-emission scanning electron microscope (FESEM, Quanta 200, Zeiss Sigma). Energy-dispersive X-ray (EDX) spectroscopy images were obtained by an EDX spectrometer (INCAPentalFETx3 Oxford). X-ray images were implemented by digital X-ray imaging system (PLX8600, Perlove Medical, China). MRI images were got by magnetic resonance imaging apparatus (Discovery MR750 3.0T, GE, America). Fluorescent microscopic images were obtained using Zeiss microscopes (AxioObserver Z1 and Axiovert 200M, Zeiss, Germany). The blood perfusion of the rabbit's central auricular artery was monitored by

Laser Doppler Flowmetry (Perimed, PeriFlux System 5010, Stockholm, Sweden). In vivo and in vitro photothermal killing experiments were carried out under 808 nm NIR laser (Hi-Tech Optoelectronics Co., Ltd, China) and the infrared thermograph (Ax5, FLIR-Systems, American).

Cell Culture. HepG2 cells and VX2 cells were cultured at 37 °C with 5% CO2 atmosphere in 89% MEM (Procell) and DMEM (HYCLONE) basal medium, respectively, supplemented with 10% fetal bovine serum (FBS, BI) and 1% Penicillin-Streptomycin solution (PS, Gibco). After the cells were grown to 80% confluence and then digested with 0.25% trypsin, resuspended in medium, and diluted to an appropriate concentration for use.

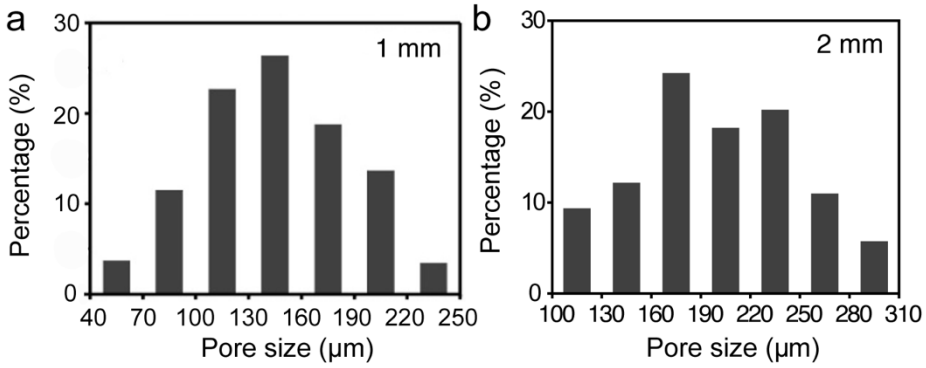

Figure S1. Pore size distribution of 3D tubular scaffold in different diameters of 1 mm (a) and 2 mm (b).

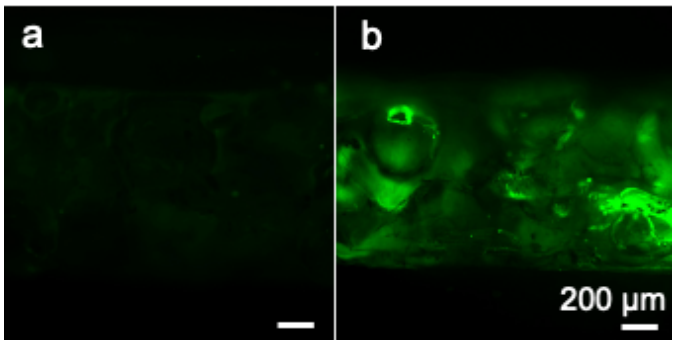

Figure S2. Characterization of anti-EpCAM antibody-functionalized 3D tubular scaffold by DyLight 488 conjugated goat anti-mouse IgG. (a) 3D tubular scaffold without modifying with anti-EpCAM antibody. (b) 3D tubular scaffold modified with anti-EpCAM antibody. Scale bars, 200 μm.

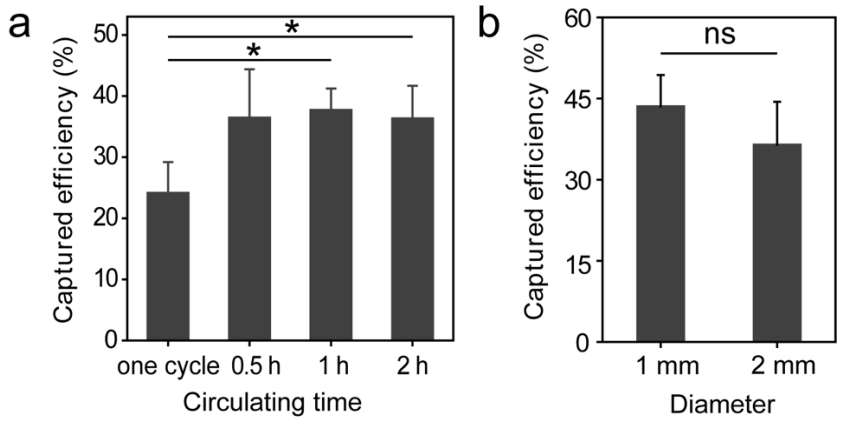

Figure S3. Cell capture performance of 3D tubular scaffold. (a) 3D tubular scaffold (2 mm diameter) with big macropores indwelled in mimic circulating system for different periods. (b) 3D tubular scaffold with small (1 mm diameter) or big (2 mm diameter) macropores indwelled in mimic circulating system for 0.5 h. Error bars, standard error (n = 3), ns $p > 0.05$, *$p < 0.05$.

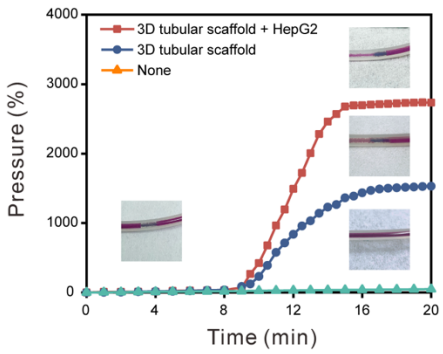

Figure S4. In vitro embolization from mimic circulating system. The curves of pressure change in vitro embolization study; insert: the start or final state of the mimic circulating system.

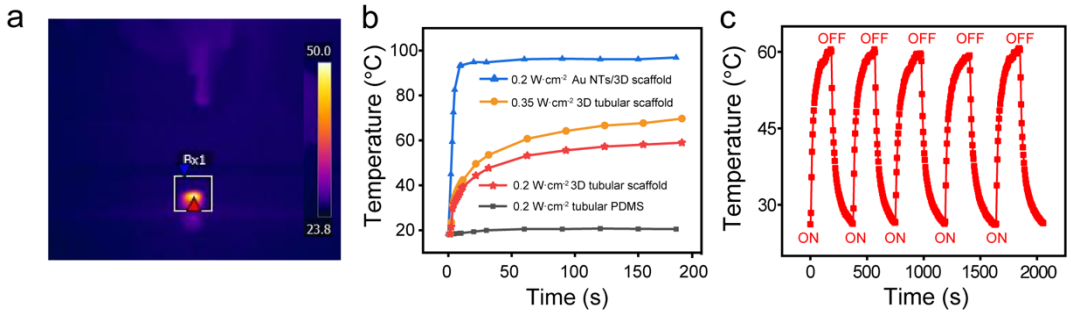

Figure S5. Photothermal performance of 3D tubular scaffold. (a) Photothermal image of 3D tubular scaffold treated by NIR laser (808 nm, 0.2 W·cm^{-2}). (b) Temperature change curves of tubular PDMS, Au NTs/3D scaffold and 3D tubular scaffold treated with NIR irradiation (808 nm, 0.2 or 0.35 W·cm^{-2}). (c) Photothermal stability of 3D tubular scaffold under five cycles of laser irradiation.

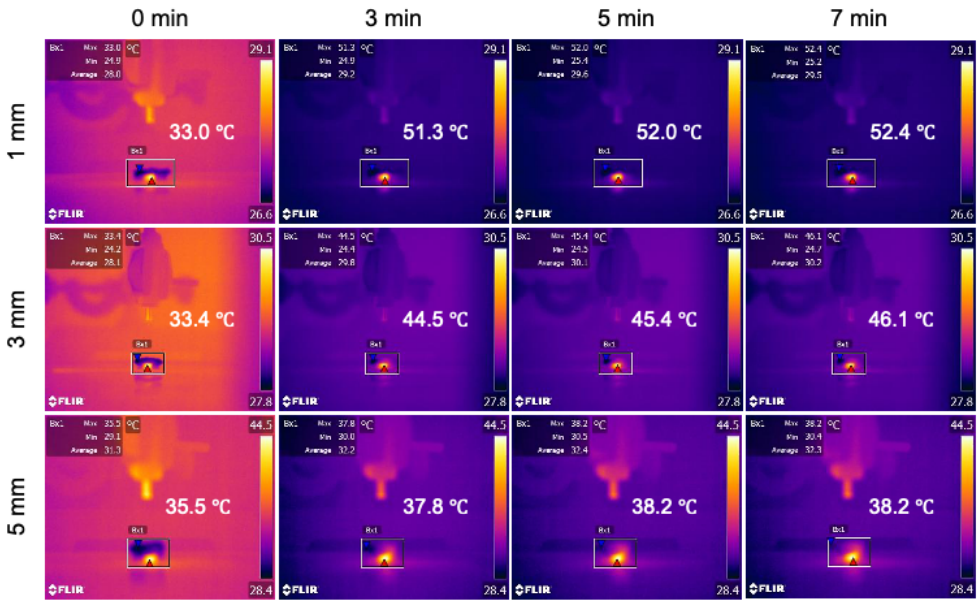

Figure S6. Photothermal sensibility test of 3D tubular scaffold. Certain thickness of pork slices was covered onto 3D tubular scaffold and then irradiated by NIR laser (808 nm, 0.2 W·cm^{-2}) for different exposure times.

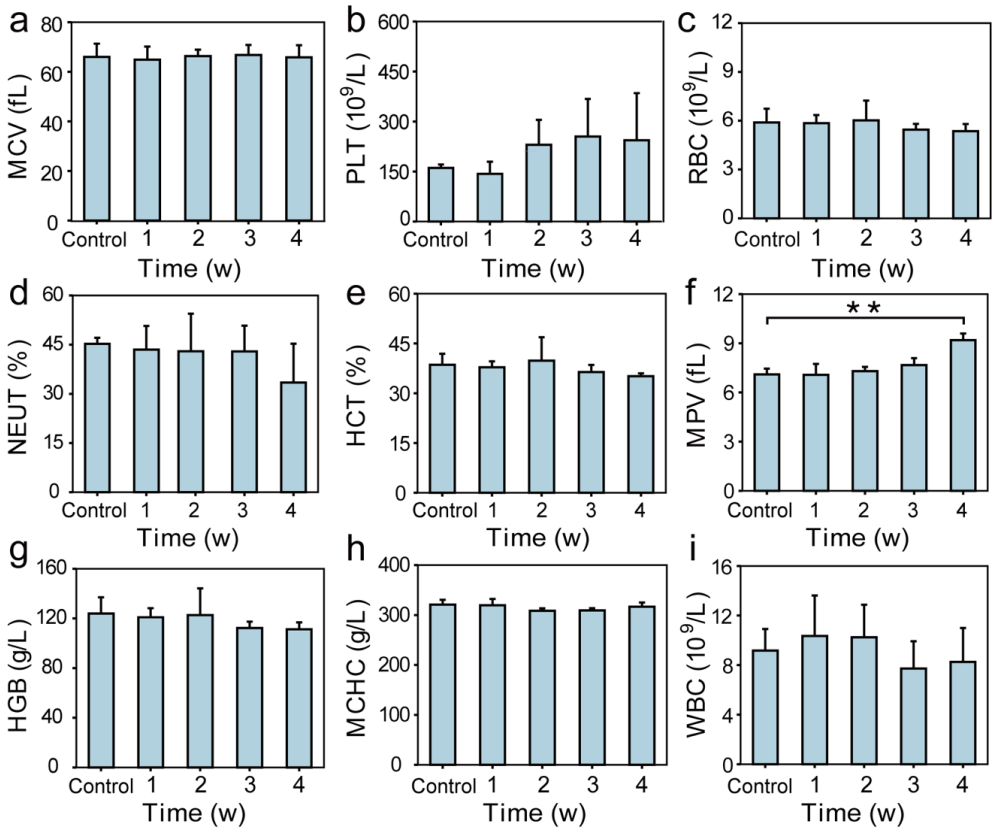

Figure S7. Blood routine examination of rabbits implanted with 3D tubular scaffold and control (none 3D tubular scaffold) groups. Error bars, standard error ($n = 3$), ns $p > 0.05$, ** $p < 0.01$.

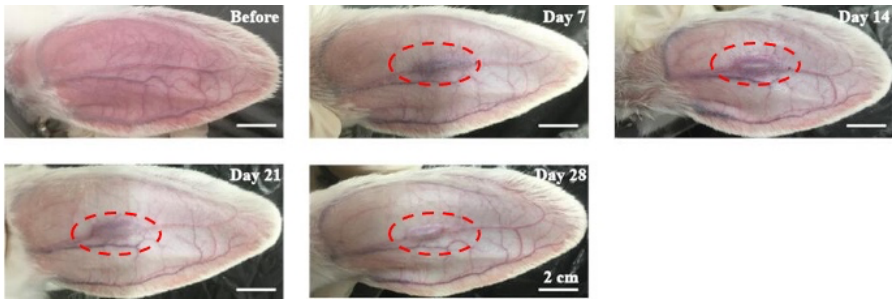

Figure S8. Photograph snapshots of rabbit ears during 28-day implantation with 3D tubular scaffold. Scale bars, 2 cm.

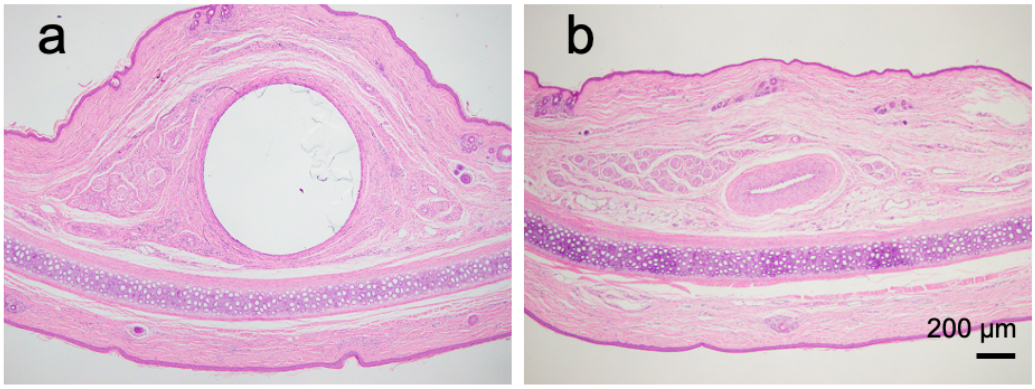

Figure S9. Morphology of rabbit auricular central artery in control and treatment group. (a) H&E staining image of rabbit auricular central artery implanted with 3D tubular scaffold. (b) H&E staining image of rabbit auricular central artery without implantation of 3D tubular scaffold (an irregular shape because of the mechanical strength during tissue slicing). Scale bar, 200 μm.

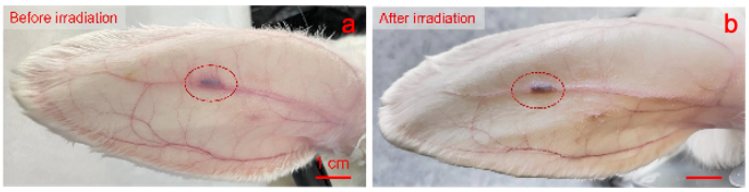

Figure S10. Photographs of rabbit ears implanted with 3D tubular scaffold before (a) and after (b) laser irradiation. Scale bars, 1 cm.

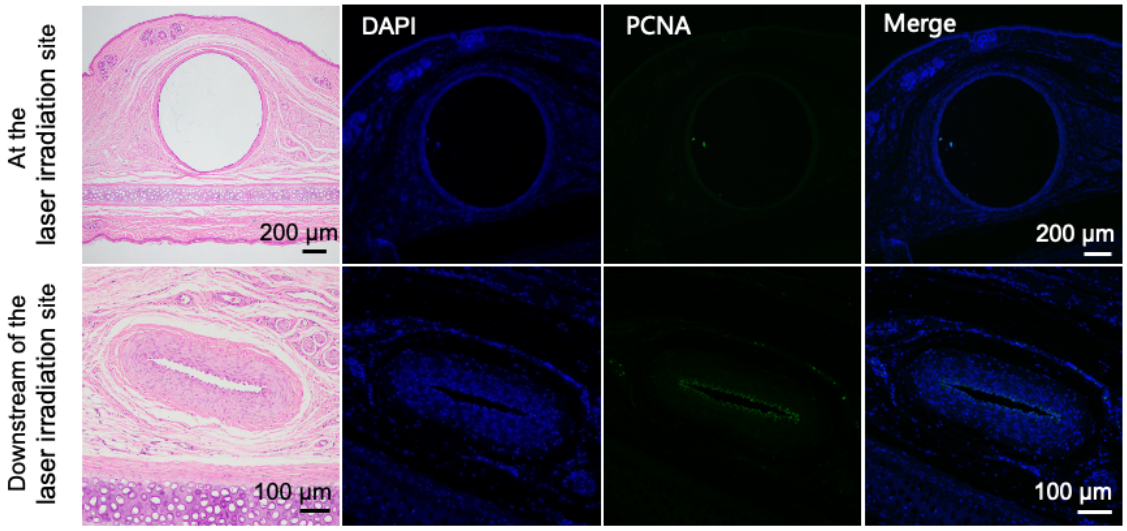

Figure S11. H&E and PCNA staining images of the ear tissues around the implantation site from rabbits implanted with 3D tubular scaffold.

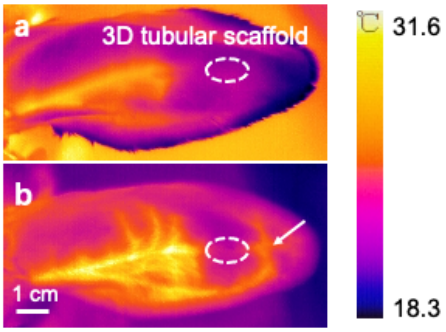

Figure S12. NIR images of rabbit ears implanted with 3D tubular scaffold before (a) and after (b) laser irradiation. Scale bars, 1 cm.

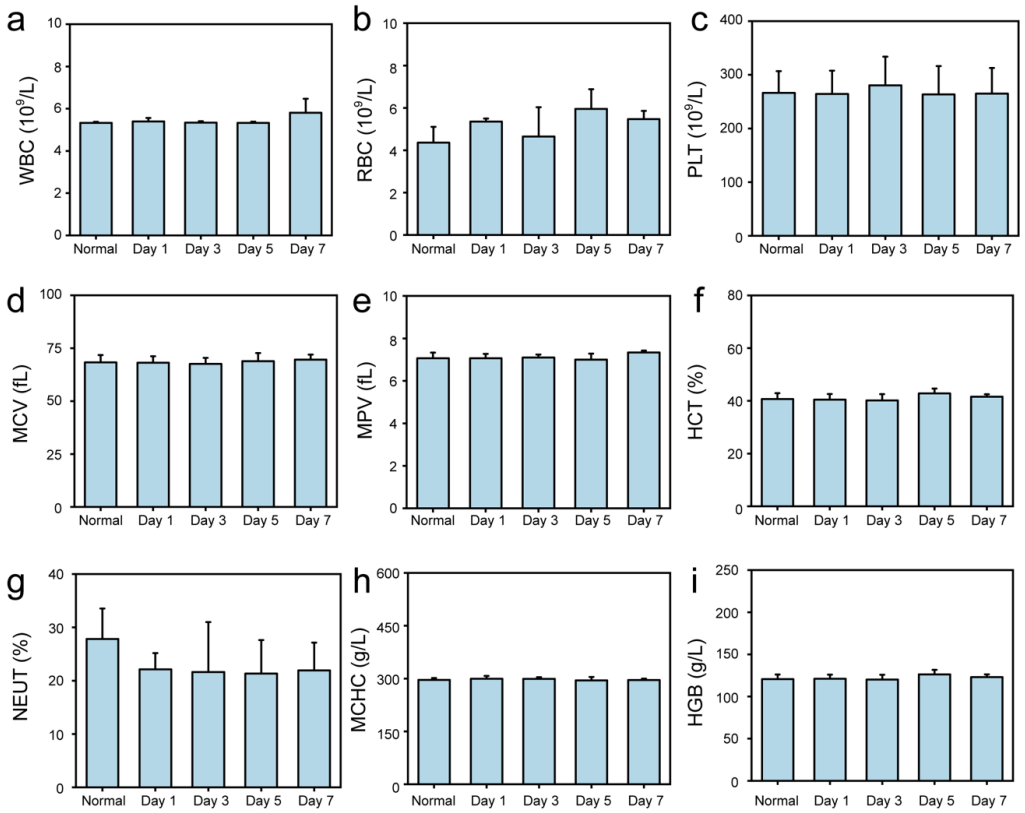

Figure S13. Blood routine examination of rabbits implanted with 3D tubular scaffold before and after laser irradiation. Error bars, standard error (n = 3).

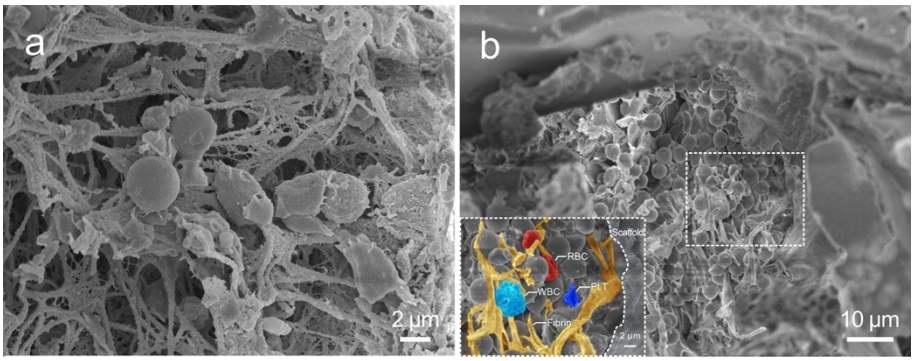

Figure S14. SEM images of 3D tubular scaffold retrieved from blood vessel after long-term indwelling. (a) 3D tubular scaffold filled with fibrin and cells. Scale bar, 2 μm. (b) The representative image presenting skeleton of 3D tubular scaffold, fibrin, and cells, simultaneously. Scale bar, 10 μm; Insert: enlarged view of selected region with marked blood cells. Scale bar, 2 μm.

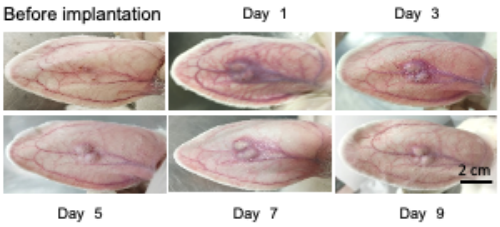

Figure S15. Photograph snapshots of tumor-bearing rabbits without implantation of 3D tubular scaffold. Scale bars, 2 cm.

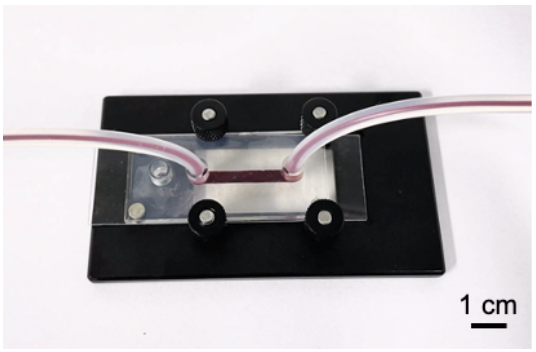

Figure S16. Photograph of the anti-EpCAM antibody-functionalized Au NTs/3D scaffold chip for CTC capture in vitro. Scale bar, 1 cm.

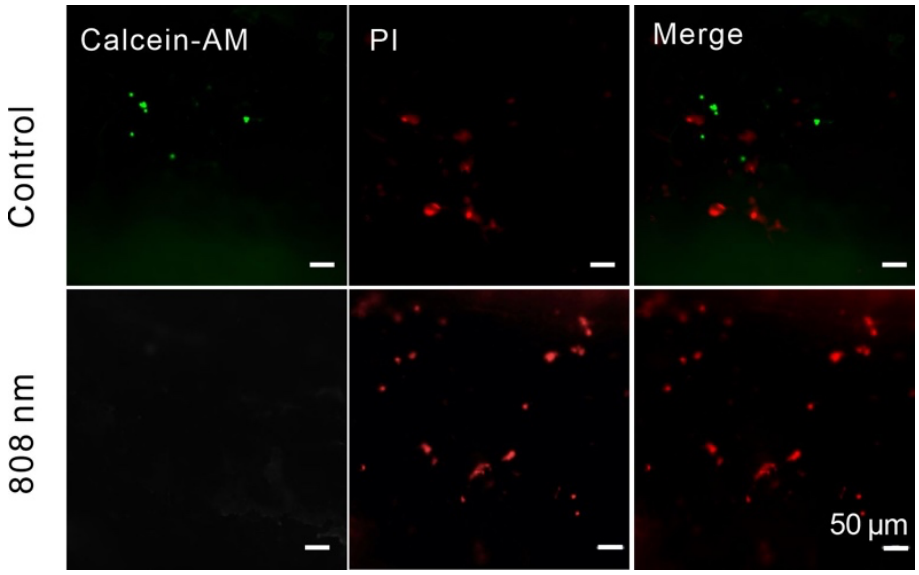

Figure S17. Cell photothermally damage capability of 3D tubular scaffold irradiated by NIR laser. Representative fluorescent images of 3D tubular scaffold in tumor-bearing rabbit irradiated by 808 nm NIR laser (0.2 W·cm^{-2}, 10 min) and then retrieved and costained by Cal-AM (green, live cells) and PI (red, dead cells). Scale bars, 50 μm.

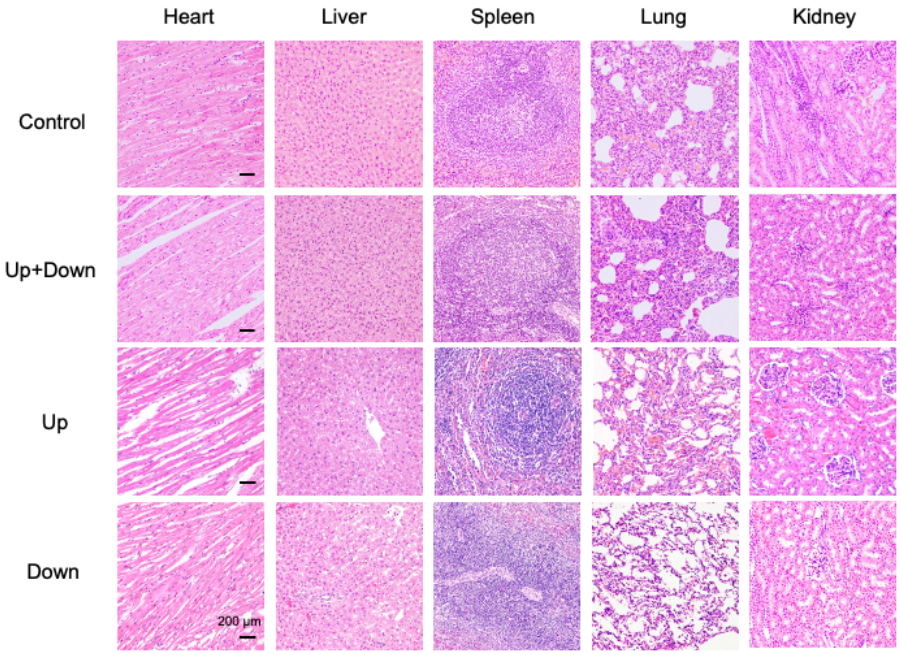

Figure S18. H&E staining images of the organs from rabbits implanted with 3D tubular scaffold and control group. Scale bars, 200 μm.

Table S1: Summarization of CTC capture efficiency of our work and other approaches.

Methods	Spiked cell number	Capture efficiency	Reference
Implantable scaffold	500	3.6±0.8%	Our work
	1000	3.7±1.4%	
	1500	3.2±0.5%	
Indwelling needle	500	4.9±1.4%	Ref. [28]
	1000	3.4±1.8%	
ZnO nanoflowers coated indwelling needle	10^5	11.0%	Ref. [45]
Intravenous catheter	10^5	2.1%	Ref. [29]
Intravascular aphaeretic system	2×10^7	0.004%	Ref. [32]
Electronic catheter	10^4	22.3% (average)	Ref. [31]